

LASER RADIATION ABSORPTION BY DENSE SODIUM VAPOR

N.I. Kosarev and I.M. Shkedov

*Siberian Aerospace Academy, Krasnoyarsk
Received June 27, 1995*

The glow of dense sodium vapor, induced by the absorbed laser radiation, has been analyzed using the methods of computer simulations. The deformation of laser pulse and frequency, angular, and spatial characteristic of a fluorescence response have been studied. Using the decrement of its attenuation, we have obtained the dependence of Biberman–Holstein capture factor on optical thickness of a medium for spherical and cylindrical geometry.

Resonance fluorescence spectroscopy is a well-known method for plasma and gas diagnostics. However, when laser radiation interacts with dense media (resonance ionization of gases,¹ optogalvanic spectroscopy,² etc.), the fluorescence response is formed in the radiative transfer mode, and the characteristics of a signal received are, as a rule, nonlinearly related to the parameters of a medium. That is why the study of the role of transfer process in the formation of a fluorescent signal is rather urgent.

In this paper we discuss the main results of numerical modeling of the process of dense sodium vapor glow under exposure to a laser pulse.

STATEMENT OF THE PROBLEM

Let the sodium vapor in a closed volume be exposed to laser radiation at $\lambda = 589 \text{ nm}$ ($S_{1/2} \rightarrow P_{3/2}$). The state of the medium is described by the balance equations for populations of two-level atoms:

$$dn_1(\mathbf{r}, t)/dt = - [k_{12} n_1(\mathbf{r}, t) - k_{21} n_2(\mathbf{r}, t)] \tilde{J}(\mathbf{r}, t) + A_{21} n_2(\mathbf{r}, t),$$

$$n_1(\mathbf{r}, 0) = n_0, \tag{1}$$

$$n_2(\mathbf{r}, t) + n_1(\mathbf{r}, t) = n_0, \quad n_2(\mathbf{r}, 0) = 0. \tag{2}$$

The radiative processes of excitation, quenching, and spontaneous decay with the characteristic time $(k_{12}\tilde{J})^{-1}$, $(k_{21}\tilde{J})^{-1}$, and A_{21}^{-1} , respectively, were taken into account. In Eqs. (1) and (2), n_0 is the initial density of atoms. The use of balance equations is based on the fact that the linewidth of laser radiation is much greater than the width of the absorption line. The intensity of radiation field, integrated over frequency and solid angles, \tilde{J} , at point \mathbf{r} is determined by the equation

$$\tilde{J}(\mathbf{r}, t) = \int_0^{2\pi} d\phi \int_0^\pi \sin\theta d\theta \int_0^\infty \Phi(\nu) I(\mathbf{r}, t, \theta, \phi, \nu) d\nu, \tag{3}$$

where $I(\mathbf{r}, t, \theta, \phi, \nu)$ is the intensity of radiation at frequency ν , propagating in the direction \mathbf{s} , determined

by angles θ and ϕ at a time t and point \mathbf{r} . It is described by the stationary transfer equation

$$dI(\mathbf{r}, t, \theta, \phi, \nu)/ds = \Phi(\nu) \chi [S - I(\mathbf{r}, t, \theta, \phi, \nu)], \tag{4}$$

since the time of radiation propagation in a medium is much smaller than the characteristic period of variation of the medium parameters. In addition, the following assumptions are made:

- 1) the model of total frequency redistribution is valid;
- 2) the scattering phase function is spherical;
- 3) an absorption line has the Doppler profile:

$$\Phi(\nu) = \frac{1}{\sqrt{\pi}} \exp\left(-\frac{(\nu - \nu_0)^2}{\Delta\nu_D^2}\right), \tag{5}$$

where $\Delta\nu_D$ is the linewidth, and ν_0 is the line center frequency;

- 4) the time–frequency shape of a laser pulse is as follows

$$I_r(\nu, t) = I_0 \frac{(\Delta\nu/2)}{(\nu - \nu_0)^2 + (\Delta\nu/2)^2} \frac{t}{\tau^*} \exp\left(1 - \frac{t}{\tau^*}\right), \tag{6}$$

where τ^* is the parameter determining the pulse length, I_0 is the intensity of laser radiation, and $\Delta\nu$ is its linewidth.

Under such assumptions, we have for the absorption coefficient χ and the source function S the following expression

$$\chi = \frac{c^2 A_{21} g_2}{8\pi\nu_0^2 g_1} [n_1(\mathbf{r}, t) - \frac{g_1}{g_2} n_2(\mathbf{r}, t)]; \tag{7}$$

$$S = \frac{2h\nu_0^3 g_2}{c^2 g_1} \frac{n_2(\mathbf{r}, t)}{n_1(\mathbf{r}, t) - \frac{g_1}{g_2} n_2(\mathbf{r}, t)}, \tag{8}$$

where c is the speed of light, h is the Planck constant, g_1 and g_2 are the statistical weights of lower and upper levels, respectively.

The boundary conditions have the following form:

$$I(\mathbf{R}_0, t, \theta, \phi, \nu) = \begin{cases} 0, & \text{if } \theta \neq 0, \\ I_r(\nu, t), & \text{if } \theta = 0, \end{cases}$$

where \mathbf{R}_0 denotes the radius–vector of the irradiated surface of vapor.

NUMERICAL METHOD

In general, the problem (1)–(9) is cylindrically symmetric because there is an isolated direction Z , related to the direction of laser pulse propagation. The procedure of discretization developed allowed us to reduce the system of equations (1)–(9) to the Cauchy problem for populations at the nodes of a specially constructed grid for the central cross section of a sphere (Fig. 1). The problem is solved numerically. The basic concepts and principles of the discretization procedure can be found in Ref. 3. They also form the basis for the algorithm of solving the problem (1)–(9) for cylindrical geometry.

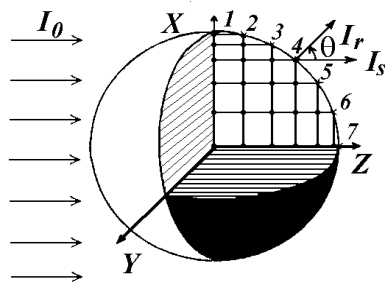


FIG. 1.

LASER PULSE ABSORPTION

The computations have been done for different values of τ^* , I_0 , and initial optical thickness τ_0 of a sphere and a cylinder. As to the latter, τ_0 was determined from the diameter of the base. The spherical geometry is convenient because within one version of computations and considering outgoing radiation at different distances from the center of a sphere, we can judge on the pulse deformation, which corresponds to paths with different optical thicknesses smaller than τ_0 .

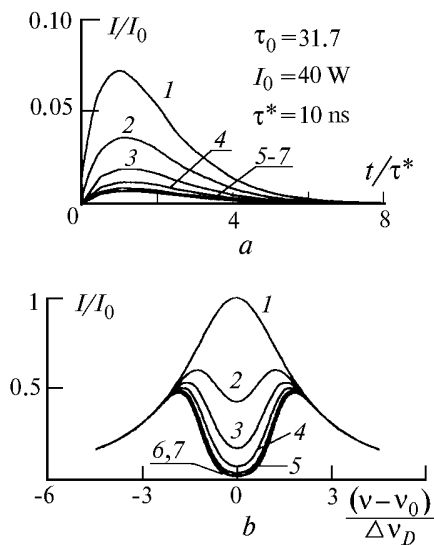


FIG. 2.

Shown in Fig. 2a is the time-dependence of outgoing radiation at the boundary points 1–7 from Fig. 1. For long optical paths, the strong absorption is observed, which results in significant deformation of the pulse shape (curves 4–7). The corresponding change of its frequency shape is shown in Fig. 2b. Naturally, the greatest absorption is noted at the central frequencies of the line profile and for paths with large optical thicknesses (curves 4–7).

The conclusions, concerning the deformation of the frequency–temporal shape of the laser pulse, are valid for a cylinder too.

GLOW OF SODIUM VAPOR

In general, the fluorescence dynamics is governed by spatial distribution of excited atoms. The distribution is formed under the action of both laser and induced radiation, with the intensity determined by the absorption coefficient χ and the source function S , respectively. Their concentration as a function of time at boundary nodes 1–7 is shown in Fig. 3 for spherical geometry and in Fig. 6 for the cylinder. The results obtained indicate that the longer is the optical path, the smaller is the number of excited atoms at its end. It is connected with the absorption of laser radiation. By comparing the curves from Fig. 3 and Fig. 2a, we draw the conclusion that the rate of decay of excited atoms is much smaller than that of laser pulse intensity at all boundary points of the medium.

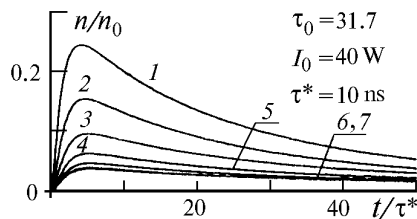
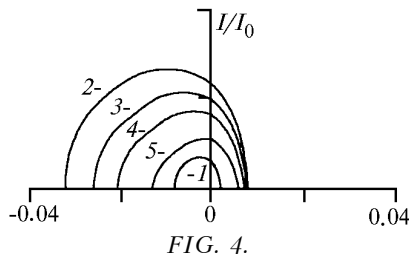


FIG. 3.

It should be noted also that the maximum in concentration of excited atoms is reached long after the maximum in intensity of laser pulse, and the longer is the path, the later appears the maximum. The delay between maxima is due to competition between processes of emission and absorption, which results in the phenomenon of radiation capture by a medium, known in spectroscopy. It manifests itself as dips at central frequencies of a line of fluorescent glow, shown in Fig. 5a, where the frequency profiles of lines are presented for different angles of observation, counted from the direction of laser pulse propagation. For small angles (0° and 45°) the dip is well pronounced (curves 1 and 2).

Angular dependence of the intensity of the glow at $\lambda = 589 \text{ nm}$ is shown in Fig. 4. Analysis of the results show that when the optical thickness of a medium is large enough, the fluorescence intensity is greater for angles above 90° than for smaller ones (as if the medium reflects). If the optical thickness is small, then

the glow is nearly isotropic, (see for example, curve 5 in Fig. 4).



It should be also noted that for an observer the apparent disk will glow inhomogeneously. This is confirmed by the data on radial dependence of the fluorescence intensity in the central cross section of a sphere at different angles of observation, shown in Fig. 5b. Similar data for cylindrical geometry are presented in Fig. 7.

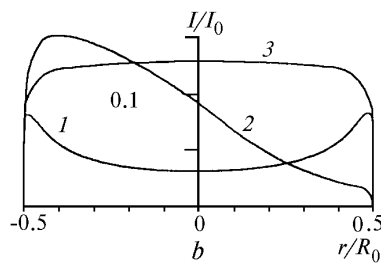
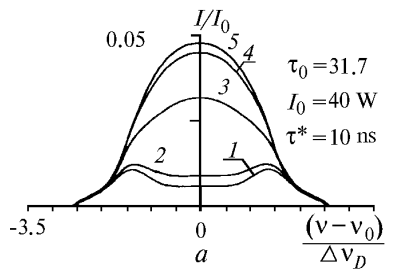


FIG. 5.

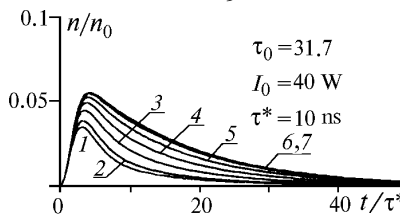


FIG. 6.

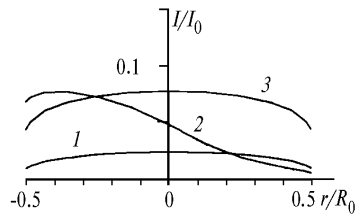


FIG. 7.

The data obtained allow the influence of the geometry on the fluorescent glow of vapor to be studied. It turns out that, although general regularities in the process of radiative transfer are retained as one goes from spherical geometry to cylindrical one,

nevertheless spatial and frequency-angular characteristics of radiation scattered can differ essentially, cf., for example, Fig. 6 with Fig. 3 and Fig. 7 with Fig. 5b.

Such a complicated pattern of the fluorescence glow is governed, first of all, by the processes of radiative transfer with regard to absorption and emission by atoms. The phenomenon of photon capture increases the effective lifetime of excited atoms. Therefore the decrement of attenuation of the fluorescent response can be used to determine the dependence of Biberman-Holstein capture factor g on optical thickness of a medium τ_0 (Fig. 8). As seen, for thicker media g factor decreases (curve 1 is for a sphere and curve 2 – for a cylinder with height-to-base diameter ratio equal to six). Its linear decrease at $\tau_0 > 4$, in a logarithmic scale (Fig. 8b), is in qualitative agreement with the experimental data,⁴ obtained for the cylindrical geometry and indicative of the validity of the Biberman-Holstein theory (curve 3). For $\tau_0 < 4$, such a dependence of g on τ , being in qualitative agreement with the experimental one, takes place, and the Biberman-Holstein theory is already invalid.

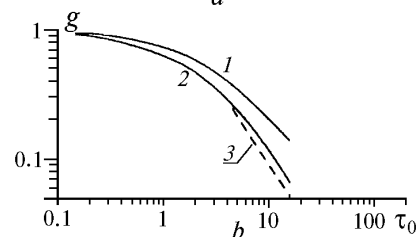
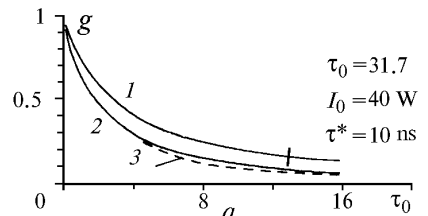


FIG. 8.

CONCLUSION

Numerical modeling of the fluorescent response from dense sodium vapor in the mode of transfer of laser pulse allowed us to obtain its spatiotemporal and frequency-angular characteristics and to determine the dependence of the capture factor on the optical thickness of a medium.

REFERENCES

1. T.B. Lucatorto and T.J. Mellrach, *Appl. Opt.* **19**, No. 23, 3948–3956 (1980).
2. N.K. Zaitsev and N.Ya. Shaparev, “*Optoelectronic phenomena in plasma*,” Preprints No. 207F, 208F, and 209F, L.V. Kirenskii Institute of Physics SB RAS, Krasnoyarsk (1982), 23, 30, and 31 pp.
3. N.I. Kosarev and I.M. Shkedov, *Atmos. Oceanic Opt.* **6**, No. 11, 744–748 (1993).
4. A. Romberg and H.-J. Kunze, *J. Quant. Spectrosc. Radiat. Transfer* **39**, No. 2, 99–107 (1988).